Proceedings Paper:
Ma, CY, Wang, XZ, Tighe, CJ et al. (1 more author) (2013) Computational Investigation of Counter-Current Reactors in a Continuous Hydrothermal Flow Synthesis System for Reactor Design Improvement. In: Bogle, D and Fairweather, M, (eds.) Computer Aided Process Engineering. 22nd European Symposium on Computer Aided Process Engineering, 17-20 Jun 2012, London, UK. Elsevier . ISBN 9780444594310

Ian David Lockhart Bogle and Michael Fairweather (Editors), Proceedings of the 22nd European Symposium on Computer Aided Process Engineering, 17 - 20 June 2012, London.

Computational Investigation of Counter-Current Reactors in a Continuous Hydrothermal Flow Synthesis System for Reactor Design Improvement

Cai Y. Ma,[a] Xue Z. Wang,[a] Christopher J. Tighe,[b] Jawwad A. Darr[b]

[a]*Institute of Particle Science and Engineering, School of Process, Environmental and Materials Engineering, University of Leeds, Leeds LS2 9JT, United Kingdom*
[b]*Department of Chemistry, University College London, London WC1H 0AJ, United Kingdom*

Abstract

Computational fluid dynamics (CFD) is applied to the study of a laboratory-scale counter-current reactor for continuous hydrothermal flow synthesis of nanomaterials. Hydrodynamic and thermodynamic variables including velocity and temperature are modelled using ANSYS Fluent package. The tracer concentration profile is also simulated via solving the species equations in order to investigate the mixing behaviour. The predicted temperatures in the counter-current reactor are found to be in good agreement with experimental data. Based on the simulation, improved designs of the reactor were proposed using shorter insertion lengths of the supercritical water tube. CFD simulation of the new designs is compared with the original reactor design, demonstrating improved mixing and heat transfer performance.

Keywords: Counter-Current Reactor, CFD, Supercritical Water, Hydrothermal Synthesis of nanomaterials

1. Introduction

Hydrothermal synthesis using supercritical water (ScW) has been used to produce numerous metal oxide particles in the nano-size range which have a wide range of applications (Lester et al., 2006). The process is relatively green since it uses water rather than organic solvents, and can be operated in either batch or continuous mode. Continuous hydrothermal flow synthesis (CHFS) method has advantages over batch mode operation (Adschiri et al., 1992). For example, it is easy to control, can avoid batch to batch variation in product quality (Boldrin et al., 2006).

In a CHFS process, reactions between ScW and metal salt take place in an impinging jet type reactor in milliseconds, followed by fast cooling. The detailed mechanism of particle formation is still not fully understood, but it was considered to involve processes of nucleation, growth, and aggregation etc. As a result, the reactor design to optimise the mixing, temperature and velocity profiles are critical. It is obviously difficult and costly to achieve the goal of optimum reactor design through experiments. Computational fluid dynamics (CFD) modelling offers a useful tool to evaluate different designs and has been used to study ScW oxidation processes (Narayanana et al., 2008). The application of CFD modelling to ScW hydrothermal synthesis for production of nanoparticles is still limited. Lester et al. (2006) used CFD technique to simulate the velocity distributions of a nozzle-type reactor. However, the simulation was based on a pseudo ScW reactor with ScW and metal salts being represented by methanol and sucrose. Aimable et al. (2009) numerically simulated the mixing zone of a reactor and

obtained the distributions of temperature and velocity but little details of the simulation were provided. Kawasaki et al. (2010) studied a T-shaped mixer for continuous ScW hydrothermal synthesis of TiO_2 nanoparticles. Various experimental conditions were simulated using CFD to understand the mixing behaviour. Sierra-Pallares et al. (2011) attempted to quantify the mixing efficiency in ScW hydrothermal reactors. The predicted results were not verified against temperature measurement. Demoisson et al. (2011) simulated a reactor operating in ScW conditions for nanomaterial formation, but only one temperature point experimentally available was compared with simulations.
In this paper, CFD models were developed for a counter-current reactor of a CHFS system. The flow and temperature profiles and mixing behaviour in the reactor were simulated using the ANSYS Fluent package (2010). The predicted temperature profiles were compared with experimental data and the mixing between ScW and precursor streams was analysed in details. The effect of insertion lengths of the ScW pipe on the reactor performance was also investigated.

2. Mathematical formulation

2.1. Hydrodynamic and concentration models

The continuity, momentum and enthalpy equations based on Reynolds averaging of the instantaneous equations are numerically solved to obtain hydrodynamic and heat transfer profiles. The widely used two-equation k - ε model (Jones and Launder, 1972) was used in this study.
Simulation of mixing was carried out by introducing a secondary liquid as an inert tracer into the reactor. The tracer concentration distributions were obtained from the solution of the Reynolds-averaged species transport equations:

$$\frac{\partial \rho Y_i}{\partial t} + \frac{\partial \rho u_j Y_i}{\partial x_j} = \frac{\partial}{\partial x_i}\left(\Gamma_{i,eff} \frac{\partial Y_i}{\partial x_j}\right) \tag{1}$$

where the effective diffusion coefficient of species i, $\Gamma_{i,eff} = \Gamma_i + \mu_t / Sc_t$, ρ is the mixture density, u_i the mixture velocity, Y_i the species mass fraction, Γ_i the species diffusion coefficient, μ_t the turbulent eddy viscosity, and Sc_t the turbulent Schmidt number.

2.2. Thermodynamic properties

In this study, the water properties obtained from National Institute of Standard and Technology (2009) using the IAPWS (International Association for the Properties of Water and Steam) formulation 1995 for the thermodynamic properties of ordinary water substance (Wagner and Pruß, 2002) were piece-wise curve-fitted in polynomial forms over several temperature ranges at 24.1 MPa, and used in the simulations. For diffusion coefficients in the mixing study, the correlation from Liu and Macedo (1995) was used to estimate the water diffusivity.

3. Experimental study

The flow diagram of the CHFS counter-current reactor system (Tighe et al., 2012) is shown in Fig. 1. Pump P1 was used to pump deionised water to 24.1 MPa at a flowrate of 20 ml/min through a heater where the water was heated to 400°C. An aqueous precursor and an aqueous base were pumped using

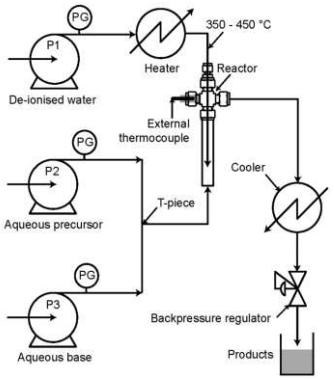

Fig. 1 Flow diagram of a counter-current CHFS system.

Pumps P2 and P3, respectively, at 24.1 MPa with a flowrate of 10 ml/min from each pump. The fluids from P2 and P3 were then mixed before entering the reactor to mix with the stream from P1, and react to generate nanoparticles. The product slurry flew upwards and left the reactor to enter a heat exchanger for rapid cooling for the collection of final product. In order to concentrate on flow, heat transfer and mixing studies of the reactor, the precursor stream was mimicked by deionised water during experiments and CFD modelling.

The reactor shown in Fig. 2(a) consists of an inner tube inserting into an outer tube with different insertion lengths (L = 45.5, 52.5, 72.5, 85.5 and 103 mm). Superheated water flows downwards in the inner tube to mix with the precursor stream (Fig. 2(a)). Product stream flows upwards to leave the reactor. Fine J-type thermocouples were inserted into the reactor at different locations along the z direction. The tips of the thermocouples were floated in the bulk flow with the estimated tip position variations being within 2 mm across the tube cross-section.

4. Simulation of the reactor

4.1. Hydrodynamic and concentration models

Figure 2(b) shows the computational domain which includes an inner tube with different insertion lengths, an outer tube, an annual channel and an exit arm. The three-dimensional domain was discretised with a typical size of 6.26×10^5 cells. The inlet conditions were taken from experiments with the inlet temperatures of ScW and precursor being 400 and 20°C, respectively. For the mixing study, a tracer with the same operating conditions and properties as the ScW was introduced into the ScW stream. Flowrates of the tracer and ScW were 1% and 99%, respectively, of the total flowrate.

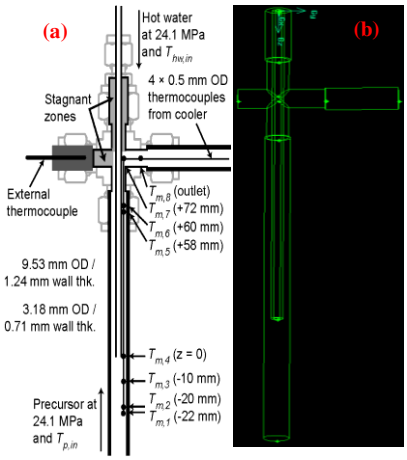

Fig. 2 (a) Diagram of a counter-current reactor; (b) Computational domain.

4.2. Solution method

The mass, momentum, energy and species equations, and the k and ε equations are solved using ANSYS Fluent (2010). The species equations were solved with the steady-state flow and temperature profiles as the initial values. SIMPLE pressure-velocity coupling was used with a second order upwind scheme being employed for the discretisation of the convection terms. The heat loss from the reactor was neglected due to the reactor insulation. The

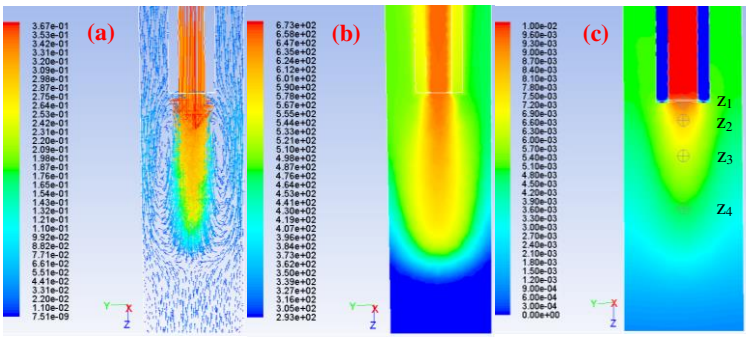

Fig. 3 Velocity vectors (a), contours of temperature (b) and tracer (c) in the ScW exit region of a counter-current reactor (L=103mm).

mass inlet flow mode was used to calculate the inlet velocities. A turbulent intensity of 10% was used for the inlet conditions for turbulence. The outlet flow mode was used for exit boundaries. Independence tests for mesh size and convergence were carried out to eliminate the effect on simulated results.

5. Results and discussion

5.1. Fluid flow and temperature profiles

Figure 3 shows the contours of velocity, temperature and tracer mass fraction distributions around the ScW exit region for case of L = 103 mm. The ScW stream penetrated into the up-coming precursor stream to form a recirculation zone surrounding the ScW jet, which enhanced the mixing between the two streams. The mixture then flew upwards through the annual channel to the product exit. Contour of tracer mass fraction at 15s after starting the transient simulation with four monitoring points (z = 103, 104, 106 and 109 mm) is shown in Fig. 3(c). The mixing times, defined as the time required for the local tracer mass fraction to reach 99% of its fully mixed mass fraction, at the four monitoring points were estimated from the predicted tracer mass fractions with values of 1.1, 2.7, 3.5 and 8.5s, respectively.

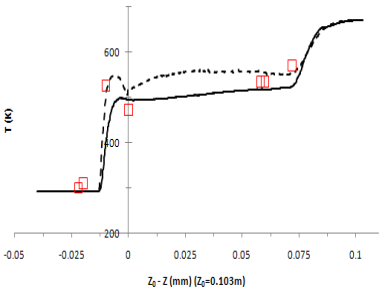

Fig. 4 Predicted (dotted line – y=1.7mm; solid line – y=2.9mm) and measured (□) temperatures along z direction (L=103mm).

The predicted and measured temperatures along the z direction are compared in Fig. 4. As the locations of the thermocouple tips can vary within 2 mm on the x-y plane in the annual section, the predicted results at y = 1.7 and 2.9 mm were plotted in Fig. 4. It can be seen that the predicted results are in good agreement with measurements, in particular for the simulated temperatures along the z direction at y = 1.7 mm, which indicated that the thermocouple tips closed to the outer wall of the inner tube.

5.2. Improvement of reactor design

With a shorter insertion length, L, the hump near the ScW exit (Fig. 4) is smaller and the ScW exit temperature (T_e) becomes higher. By monitoring the change of tracer mass fraction at point z_4 (Fig. 3), the mixing times of L = 103, 85.5, 72.5, 52.5, 45.5 mm are 8.5, 4.5, 3.5, 3.3, 3.2s, respectively, indicating that mixing is more intensive with a insertion length L ≤ 72.5 mm. The reason can be attributed to that the ScW lost more heat to the product stream in the annual channel with longer L. the ScW temperatures at the exit point (z_1) for cases of L ≤ 72.5 mm are much higher than ones for L > 72.5 mm (Fig. 5 (a)). Accordingly, much lower T_e for cases of L > 72.5 mm led to much lower exit velocity (V_e) (Fig. 5(b)), hence resulting in weaker mixing. Therefore, this study shows that the insertion length for this reactor configuration should not be longer than 72.5 mm.

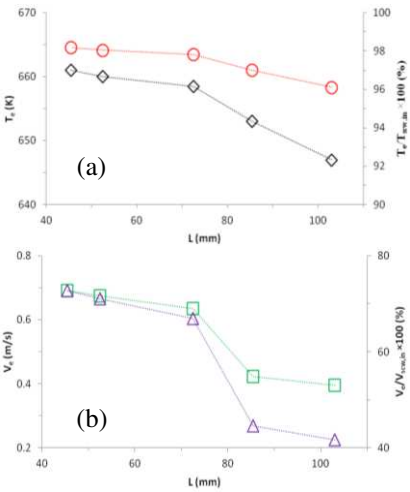

Fig. 5 Temperatures (a) and velocities (b) at the ScW exit point (z_1) under five insertion lengths (◇ – T_e; ○ – $T_e/T_{scw,in}$*100); □ – V_e; △ – $V_e/V_{scw,in}$*100).

6. Concluding remarks

In this study, CFD was used to model the flow and temperature profiles in a counter-current reactor for synthesis of nanomaterials under ScW conditions. The predicted temperatures were compared with experimental data with good agreement. The mixing study indicates that strong mixing happened in the shear layer between the recirculation zone and the ScW jet near its exit. The insertion length of the ScW tube was shortened and studied by CFD simulations with improved reactor performance being achieved.

Acknowledgements

EPSRC support for the EngNano project (EP/E040624/1 and EP/E040551/1) is acknowledged. Thanks are also due to the industrial collaborators: Johnson Matthey PLC, Corin Group PLC, Resource Efficiency Knowledge Transfer Partnership, Coates Lorilleux, AMR Technologies, Malvern Instruments and Nanoforce Technology Ltd.

References

2009. National Institute of Standard and Technology www.nist.gov.
2010. ANSYS Fluent Package www.fluent.co.uk.
T. Adschiri, K. Kanazawa, K. Arai, 1992. Rapid and continuous hydrothermal synthesis of boehmite particles in sub and supercritical water. J. Am. Ceram. Soc. 75, 2615-2618.
A. Aimable, H. Muhr, C. Gentric, F. Bernard, F. Le Cras, D. Aymes, 2009. Continuous hydrothermal synthesis of inorganic nanopowders in supercritical water: Towards a better control of the process. Powder Technol. 190, 99-106.
P. Boldrin, A.K. Hebb, A.A. Chaudhry, L. Otley, B. Thiebaut, P. Bishop, J.A. Darr, 2006. Direct synthesis of nanosized $NiCO_2O_4$ spinel and related compounds via continuous hydrothermal synthesis methods. Ind. Eng. Chem. Res. 46, 4830-4838.
F. Demoisson, M. Ariane, A. Leybros, H. Muhr, F. Bernard, 2011. Design of a reactor operating in supercritical water conditions using CFD simulations. Examples of synthesized nanomaterials. J. Supercrit. Fluids 58, 371-377.
W.P. Jones, B.E. Launder, 1972. The prediction of laminarization with a two-equation model of turbulence. Int. J. Heat Mass Transfer 15, 301–314.
S.I. Kawasaki, K. Sue, R. Ookawara, Y. Wakashima, A. Suzuki, Y. Hakuta, K. Arai, 2010. Engineering study of continuous supercritical hydrothermal method using a T-shaped mixer: Experimental synthesis of NiO nanoparticles and CFD simulation. J. Supercrit. Fluids 54, 96-102.
E. Lester, P. Blood, J. Denyer, D. Giddings, B. Azzopardi, M. Poliakoff, 2006. Reaction engineering: The supercritical water hydrothermal synthesis of nano-particles. J. Supercrit. Fluids 37, 209-214.
H.Q. Liu, E.A. Macedo, 1995. Accurate correlations for the selfdiffusion coefficients of CO_2, CH_4, C_2H_4, H_2O, and D_2O over wide ranges of temperature and pressure. J. Supercrit. Fluids 8, 310-317.
C. Narayanana, C. Frouzakisa, K. Boulouchosa, K. Prıkopsky, B. Wellig, P. Rudolf von Rohrb, 2008. Numerical modelling of a supercritical water oxidation reactor containing a hydrothermal flame. J. Supercrit. Fluids 46, 149-155.
J. Sierra-Pallares, D.L. DanieleL.Marchisio, E. Alonso, M.T. Parra-Santos, F. Castro, M.J. Cocero, 2011. Quantification of mixing efficiency in turbulent supercritical water hydrothermal reactors Chem. Eng. Sci. 66, 1576-1589.
C.J. Tighe, R.I. Gruar, C.Y. Ma, T. Mahmud, X.Z. Wang, J.A. Darr, 2012. Mixing and heat transfer in continuous hydrothermal flow synthesis reactors; An in-situ investigation of counter-current mixing. J. Supercrit. Fluids 62, 165-172.
W. Wagner, A. Pruß, 2002. The IAPWS formulation 1995 for the thermodynamic properties of ordinary water substance for general and scientific use. J. Phys. Chem. Ref. Data 31, 387-535.